

# Hypermethylation of $IFN-\gamma$ in oral cancer tissues

Songbo Tian<sup>1</sup> · Chunyang Jiang<sup>2</sup> · Xiaoqin Liu<sup>3</sup> · Sheng Xu<sup>4</sup> · Zhiyong Zhang<sup>5</sup> · Huizhen Chen<sup>5</sup> · Yinghuai Zhang<sup>5</sup> · Yanping Liu<sup>5</sup> · Dong Ma<sup>6</sup>

Received: 22 April 2016 / Accepted: 5 January 2017 / Published online: 13 January 2017  
© Springer-Verlag Berlin Heidelberg 2017

## Abstract

**Objectives** The study aimed to evaluate the methylation pattern of the interferon-gamma ( $IFN-\gamma$ ) gene in oral cancer tissues compared with normal and benign oral disease tissues.

**Materials and methods** The oral tissues were gained from the patients of 85 cases of oral squamous cell carcinoma (OSCC), 47 cases of oral dysplastic lesions, and 53 normal biopsies.  $IFN-\gamma$  methylation in oral tissues was verified through methylation-specific polymerase chain reaction (PCR) and DNA sequencing analyses, and the expression levels of  $IFN-\gamma$  messenger RNA (mRNA) and protein were detected using real-time reverse transcription (RT)-PCR and enzyme-linked immunosorbent assays, respectively.  $IFN-\gamma$  was localized in macrophages from oral tissues and detected via immunostaining.

**Results**  $IFN-\gamma$  mRNA and protein expression levels were evidently decreased in oral cancer tissues, whereas the  $IFN-\gamma$  methylation rate was significantly higher in malignant tumors

than in benign and normal tissues (normal, 22.6%; benign, 38.3%; and cancer, 55.3%;  $P < 0.05$ ). Furthermore, the expression of  $IFN-\gamma$  mRNA was significantly downregulated in oral tumors with methylation compared with tumors without methylation, as determined by real-time RT-PCR (4.76-fold difference;  $P < 0.05$ ). Likewise, mRNA expression was downregulated by 6.79-fold in oral epithelial dysplasia tissues with methylation compared with those without methylation ( $P < 0.01$ ). Co-immunostaining to detect MAC2 and  $IFN-\gamma$  demonstrated that macrophages comprised the main source of  $IFN-\gamma$  in oral tissues.  $IFN-\gamma$  methylation demonstrated a significant association with the clinical stage, histopathology grade, and primary tumor.

**Conclusions** Aberrant  $IFN-\gamma$  promoter methylation may be involved in the process of tumorigenesis of oral cancer.

**Clinical relevance**  $IFN-\gamma$  hypermethylation during the process of oral carcinogenesis could be useful for the clinical diagnosis and treatment for OSCC.

Songbo Tian, B.D., Chunyang Jiang, Xiaoqin Liu, and Sheng Xu contributed equally to this work.

✉ Chunyang Jiang  
chunyangjiang@126.com

✉ Yanping Liu  
tianyx689@sina.com

✉ Dong Ma  
mamamadong@163.com

<sup>1</sup> Department of Oral Medicine, The Second Hospital of Hebei Medical University, Heping Western Road 215, Shijiazhuang, Hebei 050000, People's Republic of China

<sup>2</sup> Department of Thoracic Surgery, Tianjin Union Medical Center, 190 Jieyuan Road, Hongqiao District, Tianjin, Tianjin 300121, People's Republic of China

<sup>3</sup> Department of Nephrology, Hongqi Hospital, Mudanjiang Medical College, 5 Tongxiang Road, Aimin District, Mudanjiang, Heilongjiang 157011, People's Republic of China

<sup>4</sup> Department of Neurosurgery, Tangshan People's Hospital, Tangshan, Hebei 063001, People's Republic of China

<sup>5</sup> Department of Physical Examination, The Second Hospital of Hebei Medical University, Heping Western Road 215, Shijiazhuang, Hebei 050000, People's Republic of China

<sup>6</sup> School of Public Health, North China University of Science and Technology, Jianshe Road 57, Tangshan, Hebei 063000, People's Republic of China

**Keywords** Oral cancer · Methylation · Cytokines · *IFN- $\gamma$*  · Tumorigenesis

## Introduction

Oral squamous cell carcinoma (OSCC), the incidence of which is increasing, is the most common type of malignant tumor of the oral cavity. Late-stage presentation of OSCC is common [1]. Recently, changes in the abundance of oral microbiota have been associated with human oral cancers [2]. Although the etiopathogenesis of OSCC appears to be complex, with interactions between genetic, environmental, lifestyle, and other factors, it is generally considered to be an immunologically mediated process characterized by the appearance of an intense band-like leukocyte infiltrate at the epithelium-connective tissue interface [3].

Immunological imbalances created by infiltrating inflammatory cells may contribute to the growth [4] and spread of oral cancer. The cytokine networks associated with several common tumors are rich in inflammatory cytokines, growth factors, and chemokines [5]. In particular, inflammatory cytokines can be produced directly by tumor cells and/or tumor-associated leucocytes and platelets that may contribute directly to malignant progression [6]. Local cytokine production within the tumor microenvironment can prevent the effector cell response [7], and cytokines can also mediate the activities of immune cells against malignant cells [8].

In humans, the cytokine interferon-gamma (*IFN- $\gamma$* ; also known as type II interferon) is critical to both the innate and adaptive immunity [9]. *IFN- $\gamma$* , the production of which is related to the induction of T lymphocyte and macrophage reactivity, maintains the major histocompatibility class II molecule expression, thus participating in keratinocyte apoptosis and oral lichen planus (OLP) disease chronicity [10] and further enhancing immune responses against malignant cells. Given the importance of *IFN- $\gamma$*  in human immune responses, it is unsurprising that genetic and epigenetic variations within *IFN- $\gamma$*  are associated with a range of diseases, including cancer [11].

Changes in DNA methylation patterns, particularly in the promoter regions of genes, can have profound effects on gene expression and have accordingly been implicated in the development of periodontal disease [12]. Methylation profiling of cancer cells and studies of individual genes have disclosed the frequent occurrence of gene-specific hypermethylation in diverse cancers (e.g., breast cancer [13] and cervical cancer [14]). Although CpG methylation of the *IFN- $\gamma$*  promoter is considered a negative transcriptional regulatory event that affects *IFN- $\gamma$*  production [15], such events have not been investigated in oral cancer tissues. Therefore, the present study aimed to evaluate the methylation status of the *IFN- $\gamma$*

promoter region in oral cancer tissues compared with that in normal and oral epithelial dysplasia tissues.

## Materials and methods

### Clinical samples and DNA extraction

The archived tissue samples from 85 cases of OSCC, 47 cases of dysplastic lesions of the oral cavity, and 53 normal biopsies were utilized in this study. Clinical characterization of the OSCC patients is summarized in Table 1. Oral tissues were collected via oral mucosa biopsy, flash-frozen in liquid nitrogen, and stored at  $-150\text{ }^{\circ}\text{C}$ . All patients provided informed consent prior to sample collection according to institutional guidelines. This protocol was approved by the ethics committee of the Second Hospital of Hebei Medical University, Shijiazhuang, Hebei Province, China.

Following the detection of malignancy, patients underwent surgical resection of primary oral cancers at the Department of Oral Surgery, Second Hospital of Hebei Medical University. The histological type and grade of each tumor was classified according to the TNM criteria set forth by the Union for International Cancer Control/American Joint Committee on Cancer, 7th edition. Tissues from samples diagnosed as dysplasia and tumorigenesis were obtained via microexcision. All primary tumor tissues and control samples were diagnosed following hematoxylin and eosin (HE) staining. Frozen tissue samples were subjected to genomic DNA extraction using standard proteinase K treatment followed by phenol/chloroform extraction. DNA concentrations were determined with a spectrophotometer.

### Bisulfite modification

Tissue methylation patterns were assessed using bisulfate-induced DNA modification in a manner similar to that reported by Goldenberg et al. [16]. In brief, bisulfite treatment converts unmethylated cytosines in DNA to uracil, whereas methylated cytosines remain unmodified. Extracted genomic DNA was modified using a bisulfite conversion kit (EZ DNA Methylation-Gold™ Kit; Zymo Research Corp.). Modified DNA was ready for immediate analysis or was stored at or below  $-20\text{ }^{\circ}\text{C}$  for later use or at or below  $-80\text{ }^{\circ}\text{C}$  for long-term storage. Each polymerase chain reaction (PCR) included 1  $\mu\text{l}$  of eluted DNA.

### Methylation-specific PCR

Methylation-specific PCR (MSP) uses specific primers for methylated or unmethylated DNA to distinguish the presence of methylation based on alterations produced after bisulfite treatment. All samples in this study were analyzed by MSP.

**Table 1** The methylation of the *IFN- $\gamma$*  gene promoter in normal oral tissue, dysplasia, and OSCC

Group	Age (years old)	Methylation ( <i>n</i> )	Methylation rate (%)
Control ( <i>n</i> = 53)	50.23 $\pm$ 7.23	12	22.6
Dysplasia ( <i>n</i> = 47)	51.07 $\pm$ 11.54	18	38.3
OSCC ( <i>n</i> = 49)	53.84 $\pm$ 9.17	27	55.1 <sup>##</sup>
<i>P</i> value	0.136 <sup>a</sup>	0.011 <sup>b</sup>	

<sup>a</sup> ANOVA test<sup>b</sup> Chi-square test\**P* < 0.05, compared with the control group; #*P* < 0.05, compared with the dysplasia group

The primer sequences for methylated and unmethylated *IFN- $\gamma$*  were described previously [14]. PCR was carried out in a total volume of 20  $\mu$ l which contained 2  $\mu$ l of bisulfite-treated genomic DNA, 1 $\times$  PCR buffer, 0.25  $\mu$ M of each primer, 250  $\mu$ M (each) dNTP mix, and 0.75 unit of FastStart Taq DNA polymerase (Roche Applied Science). Thermal cycling was initiated at 95  $^{\circ}$ C for 5 min, followed by 40 cycles of 95  $^{\circ}$ C for 30 s; specific annealing temperature for 30 s; extension temperature at 72  $^{\circ}$ C for 30 s; and a final extension at 72  $^{\circ}$ C for 2 min. An untreated blood DNA from a normal individual was used as a negative control. A methylation-positive DNA control was made in vitro using SssI methylase (New England Biolabs, Beverly, MA, USA) which methylated every cytosine of CpG dinucleotide in the DNA. Water blanks were included with each assay. The same PCR conditions were used for tumor, dysplasia, and normal tissue DNA. PCR products were visualized on 2% agarose gels stained with ethidium bromide. Positive amplification only of unmethylated primers was interpreted as unmethylation. Positive amplification only of methylated primers or both methylated and unmethylated primers was defined as methylation.

### Direct sequencing

Methylated and unmethylated PCR products were confirmed by direct sequencing. PCR products were gel purified and analyzed on an automated DNA sequence analyzer (ABI 3730x1, Life Technologies, Carlsbad, CA, USA) with a BigDye<sup>®</sup> Terminator kit (Life Technologies).

### IFN- $\gamma$ messenger RNA determination

Total RNA was extracted from the OSCC, dysplastic lesions, and normal tissues, which were homogenized with gentle MACS<sup>™</sup> Dissociator (Miltenyi Biotec) using the TRIzol (Invitrogen) according to the manufacturer's instructions. The quality of the RNA was determined using a BioSpectrometer (Eppendorf). One microgram of RNA was subjected to reverse transcription using a first-strand cDNA synthesis kit (Invitrogen) according to the manufacturer's instructions. RT-qPCR of messenger RNAs (mRNAs) was

performed using a Platinum SYBR Green qPCR Super Mix UDG Kit (Invitrogen), and real-time PCR experiments were carried on an ABI 7500 FAST system (Life Technologies). Primer sequences for *IFN- $\gamma$*  were described previously [14]. A relative amount of transcripts was normalized with  $\beta$ -actin and calculated using the  $2^{-\Delta\Delta C_t}$  formula. All real-time RT-PCRs were performed in triplicate.

### Immunohistochemistry

Tissue samples were dehydrated in an ethanol series, cleared in xylene, and embedded in paraffin. Four-micrometer r sections were prepared and mounted on poly-L-lysine-coated slides. Immunohistochemical analysis was done using a commercially available kit (Invitrogen, Carlsbad, CA, USA). Sections were incubated at 60  $^{\circ}$ C for 30 min and deparaffinized in xylene. Endogenous peroxidase activity was quenched by incubation in a 9:1 methanol/30% hydrogen peroxide solution for 10 min at room temperature. Sections were rehydrated in PBS (pH 7.4) for 10 min at room temperature. Sections were then blocked with 10% normal serum for 10 min at room temperature followed by incubation with anti-*IFN- $\gamma$*  antibodies (Proteintech) at a dilution of 1:100 for 16 h at room temperature. After washing thrice in PBS, the sections were incubated with secondary antibody conjugated to biotin for 10 min at room temperature. After additional washing in PBS, the sections were incubated with streptavidin-conjugated horseradish peroxidase enzyme for 10 min at room temperature. Following final washes in PBS, antigen-antibody complexes were detected by incubation with a hydrogen peroxide substrate solution containing a aminoethylcarbazole chromogen reagent. Slides were rinsed in distilled water, coverslipped using aqueous mounting medium, and allowed to dry at room temperature. The relative intensities of the completed immunohistochemical reactions were evaluated using light microscopy by three independent, trained observers who were unaware of the clinical data. All areas of tumor cells within each section were analyzed. All tumor cells in ten random high-power fields were counted. A scale of 0 to 3 was used to score relative intensity, with 0 corresponding to no detectable immunoreactivity and 1, 2, and 3 equivalent to low, moderate, and high staining, respectively.

## Immunofluorescence

Immunofluorescence staining was performed with 4- $\mu$ m paraffin cross sections from the OSCC tissues ( $n = 85$ ), dysplastic lesions of the oral tongue tissues ( $n = 47$ ), and normal tongue tissues ( $n = 53$ ). After deparaffinized with xylene and rehydrated, the slides were pre-incubated with 10% normal goat serum (710027, KPL) and then incubated with primary mouse monoantibody anti-*MAC2* (60207-1, Proteintech) and rabbit polyantibody anti-*IFN- $\gamma$*  (18013-1, Proteintech). Secondary antibodies were a fluorescein-labeled antibody to mouse IgG (021815, KPL) and a rhodamine-labeled antibody to rabbit IgG (031506, KPL). In each experiment, DAPI (157574, MB Biomedical) was used for nuclear counter staining. Images were captured by confocal microscopy (DM6000 CFS, Leica) and processed by LAS AF software.

## Enzyme-linked immunosorbent assay

Enzyme-linked immunosorbent assay (ELISA) (Total Survivin TiterZyme<sup>®</sup> Enzyme Immunometric Assay; Assay Designs, Ann Arbor, MI, USA) was used to determine the *IFN- $\gamma$*  levels in tissue protein extracts of samples from patients with OSCC ( $n = 85$ ), dysplasia ( $n = 47$ ), and control tissues ( $n = 53$ ). The undiluted samples were loaded in duplicate onto a 96-microtiter plate coated with antihuman *IFN- $\gamma$*  monoclonal antibody. To quantify the *IFN- $\gamma$*  concentrations, a standard curve of increasing quantities of purified recombinant *IFN- $\gamma$*  was created for each experiment. After incubation at room temperature on a plate shaker for 1 h at 500 rpm, excess sample or standard was washed out, and a rabbit polyclonal antibody specific for *IFN- $\gamma$*  was added. After another 1-h incubation, the excess antibody was washed out and a HRP-conjugated goat anti-rabbit IgG antibody was added. The excess conjugate was washed out after a 30-min incubation, after which 3,3',5,5'-tetramethylbenzidine substrate solution was added to induce the colorimetric reaction. After another 30-min incubation, the enzymatic reaction was stopped and the plate absorbance was immediately read at 450 nm. The measured optical densities were directly proportional to the concentrations of *IFN- $\gamma$*  for both the standards and samples.

## Statistical analysis

Data are presented as means  $\pm$  standard errors of the mean. One-way ANOVA was used to assess the association of gene expression with histopathological parameters. Student's *t* test was used to compare the parametric data between groups. An analysis of variance and Bonferroni's post test were used to compare multiple groups. A *P* value  $<0.05$  was considered statistically significant. All statistical analyses were performed with SPSS 13.0 (SPSS, Inc., Chicago, IL, USA).

## Results

### *IFN- $\gamma$* mRNA and protein levels correlate with oral tumorigenesis

Although RT-PCR detected *IFN- $\gamma$*  mRNA expression in control, dysplasia, and OSCC tissues, the expression was obviously decreased in oral cancer tissues (Fig. 1a). *IFN- $\gamma$*  staining was markedly decreased in OSCC tissues versus controls and dysplasia tissues via immunohistochemistry (Fig. 1b). ELISA was used to quantify *IFN- $\gamma$*  protein expression in control, dysplasia, and OSCC tissues. Notably, the *IFN- $\gamma$*  protein level was modestly increased in dysplasia tissues compared with control tissues, whereas a more robust reduction was observed in oral cancer tissues, consistent with the results of the PCR analysis (Fig. 1b, c).

### The *IFN- $\gamma$* promoter region is frequently methylated in human oral carcinomas

Epigenetic changes in cytokine genes can affect the ability of a cell to express these genes [17]. In human tumors, aberrant promoter region methylation causes the loss of expression of many cytokine genes [18]. To determine whether the *IFN- $\gamma$*  promoter is hypermethylated in human oral carcinomas under physiological conditions, we isolated genomic DNA from 85 primary tumor specimens derived from human patients with oral cancer, 47 dysplasia specimens derived from human patients with oral dysplasia, and 53 normal specimens. MSP analysis revealed methylation of the *IFN- $\gamma$*  promoter in 55.3% (47/85) primary oral carcinoma specimens, whereas only 38.3% (18/47) of dysplasia specimens and 22.6% (12/53) of normal specimens exhibited methylation (shown in Table 2). Aberrant *IFN- $\gamma$*  promoter methylation and representative bands from the MSP analysis of *IFN- $\gamma$*  are presented in Fig. 2a, c.

### DNA sequencing of MSP products

MSP products from the methylated DNA of control, dysplasia, and oral cancer samples were subjected to DNA sequencing, which yielded the expected nucleotide changes in control samples. The representative results of a bisulfite sequence analysis of the *IFN- $\gamma$*  promoter are shown in Fig. 2b. One CpG site was observed in the amplicon after excluding the primer sites.

### Transcriptional activation in response to *IFN- $\gamma$* methylation in oral tissues

Real-time RT-PCR was used to detect mRNA expressions and, thus, the effect of *IFN- $\gamma$*  promoter methylation on transcriptional silencing in different groups. Oral tumors with

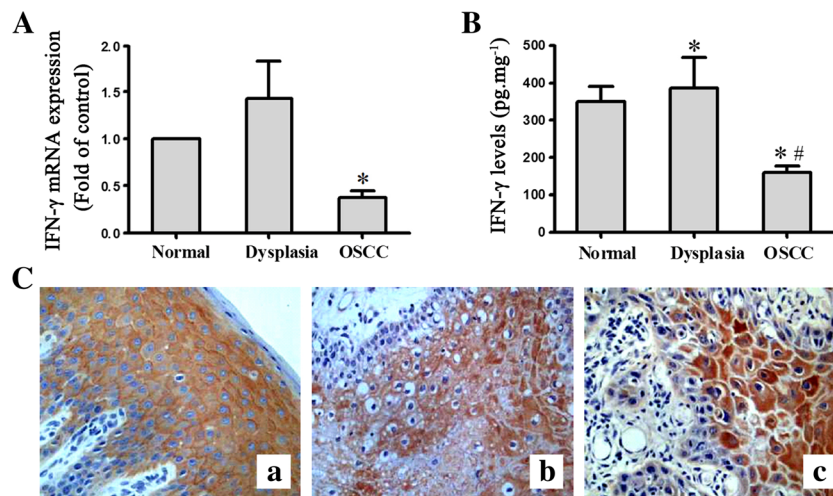


**Fig. 1** Oral tumorigenic tissues express relatively low levels of *IFN-γ* mRNA and protein. **a** Real-time reverse transcription polymerase chain reaction demonstrated differences in *IFN-γ* mRNA expression levels between groups. \* $P < 0.05$  and # $P < 0.01$  compared with dysplasia samples. **b** *IFN-γ* protein levels in control ( $n = 53$ ), dysplasia ( $n = 47$ ), and oral squamous cell carcinoma (OSCC) tissues ( $n = 85$ ) were analyzed

via enzyme-linked immunosorbent assay. **c** Paraffin-embedded tissue sections were prepared from matched pairs of human primary OSCC, dysplasia, and normal tissues and were subjected to immunohistochemistry with an *IFN-γ*-specific antibody. Representative images of *IFN-γ* staining in human normal tissue (a), dysplasia tissue (b), and primary OSCC (c) are shown. Scale bars = 50 μm

**Table 2** Relationship between methylation status of the *IFN-γ* gene and clinicopathological characteristics in OSCC tissues

	Patients with methylated samples <i>IFN-γ</i> (%) ( $n = 31$ )	Patients with unmethylated samples <i>IFN-γ</i> (%) ( $n = 18$ )	<i>P</i> value
<b>Gender</b>			
Female	13	6	0.388
Male	18	12	
<b>Age (years)</b>			
≥50	15	7	0.366
<50	16	11	
<b>Clinical stages</b>			
I + II	10	12	0.021
III + IV	21	6	
<b>Histopathology grade</b>			
Well	11	13	0.014
Poor/moderate	20	5	
<b>Regional lymph nodes</b>			
N0	12	11	0.112
N+	19	7	
<b>Distant metastasis</b>			
M0	29	17	0.698
M1	2	1	
<b>Primary tumor</b>			
T1	12	13	0.024
T2–T4	19	5	
<b>Muscle invasion (tongue)</b>			
No	13	10	0.266
Yes	18	8	
<b>Depth of muscle invasion (tongue) (mm)</b>			
<4	15	12	0.173
≥4	16	6	



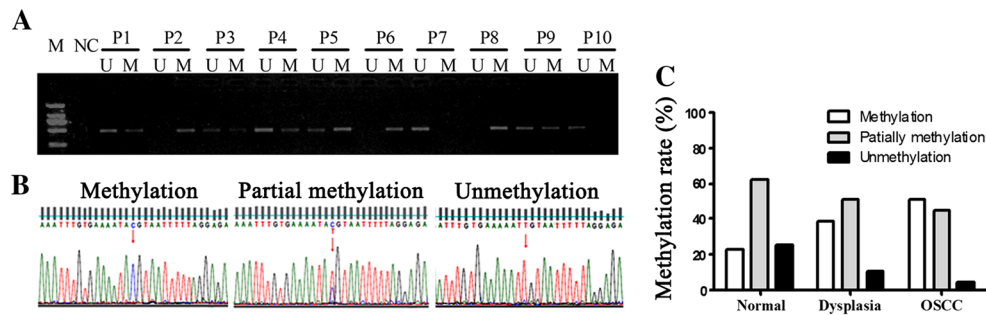


**Fig. 2** Methylation status polymerase chain reaction analysis of *IFN- $\gamma$*  in human oral tissues. **a** *IFN- $\gamma$*  methylation statuses of human primary oral squamous cell carcinoma (OSCC), dysplasia, and normal specimens. Representative bands are shown. *P1–P3* were derived from 85 patients with oral cancer, *P4–P7* from 47 patients with dysplasia, and *P8–P10* from 53 normal controls. Genomic DNA was modified with sodium

bisulfite as described in the “Materials and methods” section and analyzed via methylation status polymerase chain reaction with unmethylation (U) and methylation (M) primers. **b** Sequencing of *IFN- $\gamma$*  with representative data indicating partial and total CpG methylation. **c** *IFN- $\gamma$*  methylation rates in normal ( $n = 53$ ), dysplasia ( $n = 47$ ), and OSCC ( $n = 85$ ) tissues

methylation exhibited significantly downregulated (4.76-fold) *IFN- $\gamma$*  mRNA expression compared with those without methylation ( $P < 0.01$ ). Likewise, oral epithelial dysplasia tissues with methylation exhibited considerably downregulated mRNA expression compared with those without methylation (6.79-fold difference;  $P < 0.01$ ; Fig. 3a, b).

#### *IFN- $\gamma$* expression in macrophages from oral tissues

Given that macrophages might comprise a main source of *IFN- $\gamma$*  in tumors, we investigated the expression of *IFN- $\gamma$*  in macrophages involved in oral cancers via dual immunofluorescence staining of human oral tissue sections to determine *IFN- $\gamma$*  and Mac-2 expression. Our results showed a significant reduction in the mean percentage of *IFN- $\gamma$* <sup>+</sup> Mac-2-positive cells in oral cancer tissues compared with controls ( $1.3 \pm 0.31$  vs.  $3.2 \pm 0.11$ ,  $P < 0.01$ ). In contrast, we observed a significant increase in this cell population in oral epithelial dysplasia tissues ( $6.2 \pm 1.1$  vs.  $3.2 \pm 0.11$  for controls,  $P < 0.05$ ; Fig. 4a, b).

#### Clinicopathological features and *IFN- $\gamma$* hypermethylation in oral cancer

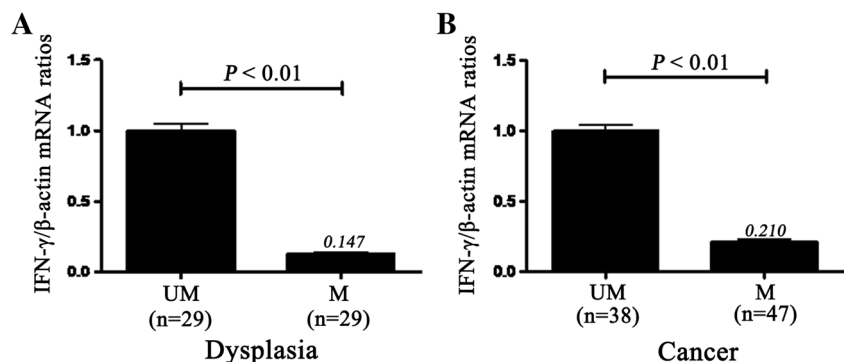
The results of a methylation status-based multivariate analysis of the *IFN- $\gamma$*  promoter regions in oral cancer tissues are shown

in Table 2. The evaluated clinicopathological parameters included sex, age, clinical stage, histopathology grade, regional lymph node involvement, distant metastasis, primary tumor scale, muscle invasion, and depth of muscle invasion (tongue). *IFN- $\gamma$*  methylation was found to associate significantly with the clinical stage ( $P = 0.021$ ), histopathology grade ( $P = 0.014$ ), and primary tumor ( $P = 0.024$ ). However, *IFN- $\gamma$*  methylation had no apparent associations with sex ( $P = 0.830$ ), age ( $P = 0.827$ ), regional lymph node involvement ( $P = 0.280$ ), distant metastasis ( $P = 0.456$ ), muscle invasion ( $P = 0.517$ ), and depth of muscle invasion ( $P = 0.220$ ).

#### Discussion

In tumor cells, gene expression is frequently regulated by epigenetic events [19]. In the present study, we evaluated the methylation patterns and expression of *IFN- $\gamma$*  in histologically confirmed biopsies from patients with premalignant and malignant oral lesions. Our findings demonstrated hypermethylation of *IFN- $\gamma$*  in most oral cancer tissues and, correspondingly, low levels of *IFN- $\gamma$*  expression compared with control samples. In addition, we determined an association between oral carcinogenesis and DNA methylation in the *IFN- $\gamma$*  promoter region.

**Fig. 3** *IFN- $\gamma$*  CpG methylation and mRNA expression in oral tissues. *IFN- $\gamma$*  mRNA expression was detected using quantitative real-time reverse transcription polymerase chain reaction (PCR) in oral dysplasia (a) and cancer tissues (b). M and UM indicate methylation and unmethylation, respectively.  $P < 0.01$  versus UM



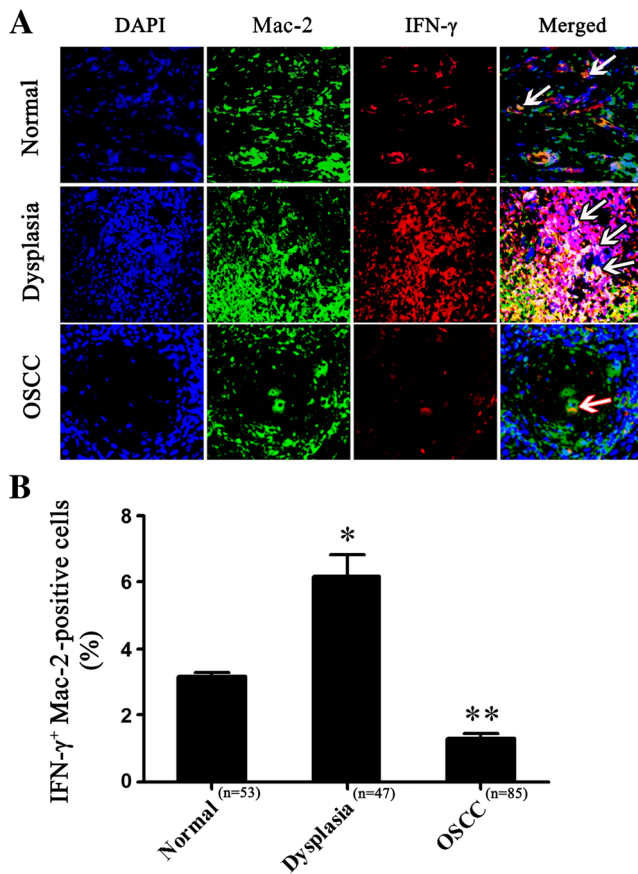


**Fig. 4** Coexpression of *IFN-γ* and Mac-2 in human oral cancer tissues. **a** Sections from human normal, dysplasia, and OSCC specimens were subjected to immunofluorescent staining. Red, green, and blue staining indicates *IFN-γ*, Mac-2, and DAPI (nuclei), respectively (scale bars = 50 μm). **b** Analysis of *IFN-γ* expression in Mac-2-positive cells from human oral cancer tissues as determined via immunofluorescence. Arrows indicate *IFN-γ*-positive macrophages. \**P* < 0.05 versus normal; \*\**P* < 0.05 versus dysplasia

To verify this hypothesized epigenetic regulation of *IFN-γ* production, gene transcription in each group was evaluated according to the MSP status. In the present study, we observed obvious decreases in *IFN-γ* mRNA and protein expression and a significant increase in *IFN-γ* methylation in oral cancer tissues. Notably, the methylated samples expressed lower levels of *IFN-γ* mRNA than the unmethylated samples in both the dysplasia and cancer groups. These data suggest that the decreased production of *IFN-γ* via the hypermethylation and silencing of its gene promoter promotes inflammation.

*IFN-γ*, which may control tumor cell immunogenicity via its selective production in the tumor microenvironment, has been shown to be a crucial component of the cancer immunoediting process [20]. Tumor-associated macrophages have been shown to exert both positive and negative effects on tumor growth in various types of cancer [21]. Therefore, delineation of the specific contributions of macrophages and related cytokines to oral tumorigenesis is a key to an understanding of oral cancer. Through our detection of *IFN-γ*

expression in macrophages from human oral tissues, we observed a loss of *IFN-γ* expression in oral cancer tissues compared with control and dysplasia tissues, without a corresponding change in the number of macrophages. This suggests that future studies will be required to identify the biological effects of *IFN-γ* silencing by methylation and their relationship in macrophages to the malignant phenotype.

In this study, *IFN-γ* methylation did not associate with prognostic variables, such as sex, age at diagnosis, regional lymph node involvement, distant metastasis, muscle invasion (tongue), and depth of muscle invasion (tongue). However, *IFN-γ* methylation significantly correlated with the clinical stage (*P* = 0.021), histopathology grade (*P* = 0.014), and primary tumor (*P* = 0.024), indicating that *IFN-γ* exerts a significant influence on the growth and differentiation of both normal and malignant oral epithelia.

To summarize, hypermethylation-induced transcriptional silencing of *IFN-γ* in both premalignant and malignant oral lesions induces expression patterns distinct from those in the normal oral mucosa and suggests an important role for these changes in the progression from a premalignant state to malignancy. The detection and quantitation of promoter region methylation could facilitate clinical p T category of OSCC and contribute significantly to the screening, surveillance, and management of premalignant oral lesions and OSCC. Thus, aberrant *IFN-γ* promoter methylation could be related with tumorigenesis of oral cancer.

**Compliance with ethical standards**

**Conflict of interest** The authors declare that they have no competing interests.

**Funding** This work was supported by grants from the National Nature Science Foundation of China (No. 81541149) and the Tianjin health and Tianjin Health and Family Planning Commission of Science and Technology Project Foundation (No. 16KG153).

**Ethical approval** All procedures performed in studies involving human participants were in accordance with the ethical standards of the institutional research committee of the Second Hospital of Hebei Medical University, Shijiazhuang, Hebei Province, China, and with the 1964 Helsinki Declaration and its later amendments or comparable ethical standards.

**Informed consent** Informed consent was obtained from all individual participants included in the study.

**References**

1. Brocklehurst P, Kujan O, O'Malley LA et al (2013) Screening programmes for the early detection and prevention of oral cancer. *Cochrane Database Syst Rev* 11:CD004150
2. Schmidt BL, Kuczynski J, Bhattacharya A et al (2014) Changes in abundance of oral microbiota associated with oral cancer. *PLoS One* 9:e98741

3. Bagan JV, Scully C (2008) Recent advances in oral oncology 2007: epidemiology, aetiopathogenesis, diagnosis and prognostication. *Oral Oncol* 44:103–108
4. Lin WW, Karin M (2007) A cytokine-mediated link between innate immunity, inflammation, and cancer. *J Clin Invest* 117: 1175–1183
5. Smyth MJ, Cretney E, Kershaw MH et al (2004) Cytokines in cancer immunity and immunotherapy. *Immunological Rev* 202: 275–293
6. Lin EY, Pollard JW (2004) Role of infiltrated leucocytes in tumor growth and spread. *Br J Cancer* 90:2053–2058
7. Venetsanakos E, Beckman I, Bradley J et al (1997) High incidence of interleukin 10 mRNA but not interleukin 2 mRNA detected in human breast tumours. *Br J Cancer* 75:1826–1830
8. Mocellin S, Wang E, Marincola FM (2001) Cytokines and immune response in the tumor microenvironment. *J Immunother* 24:392–407
9. Schoenborn JR, Wilson CB (2007) Regulation of interferon-gamma during innate and adaptive immune responses. *Adv Immunol* 96:41–101
10. Sugeran PB, Savage NW, Walsh LJ et al (2002) The pathogenesis of oral lichen planus. *Crit Rev Oral Biol Med* 13:350–365
11. Smith NL, Denning DW (2014) Clinical implications of interferon- $\gamma$  genetic and epigenetic variants. *Immunology* 143: 499–511
12. Viana MB, Cardoso FP, Diniz MG et al (2011) Methylation pattern of IFN- $\gamma$  and IL-10 genes in periodontal tissues. *Immunobiology* 216:936–941
13. Cho YH, Shen J, Gammon MD et al (2012) Prognostic significance of gene-specific promoter hypermethylation in breast cancer patients. *Breast Cancer Res Treat* 131:197–205
14. Ma D, Jiang C, Hu X et al (2014) Methylation patterns of the IFN- $\gamma$  gene in cervical cancer tissues. *Sci Rep* 4:6331–6331
15. Lovinsky-Desir S, Ridder R, Torrone D et al (2014) DNA methylation of the allergy regulatory gene interferon gamma varies by age, sex, and tissue type in asthmatics. *Clin Epigenetics* 6:9
16. Goldenberg D, Harden S, Masayeva BG et al (2004) Intraoperative molecular margin analysis in head and neck cancer. *Arch Otolaryngol Head Neck Surg* 130:39–44
17. Sanders VM (2006) Epigenetic regulation of Th1 and Th2 cell development. *Brain Behav Immun* 20:317–324
18. Esteller M (2005) Aberrant DNA methylation as a cancer-inducing mechanism. *Annu Rev Pharmacol Toxicol* 45:629–656
19. Kerr KM, Galler JS, Hagen JA et al (2007) The role of DNA methylation in the development and progression of lung adenocarcinoma. *Dis Markers* 23:5–30
20. Grivennikov SI, Greten FR, Karin M (2010) Immunity, inflammation, and cancer. *Cell* 140:883–899
21. Mantovani A, Allavena P (2015) The interaction of anticancer therapies with tumor-associated macrophages. *J Exp Med* 212:435–445